

RH: Phylogenetic analysis of host repertoire evolution

Bayesian inference of ancestral host-parasite interactions under a phylogenetic model of host repertoire evolution

MARIANA P BRAGA¹, MICHAEL LANDIS², SÖREN NYLIN¹, NIKLAS JANZ¹ AND FREDRIK RONQUIST³

¹*Department of Zoology, Stockholm University, Stockholm, SE-10691, Sweden;*

²*Department of Ecology and Evolution, Yale University, New Haven, CT, 06511, USA;*

³*Department of Bioinformatics and Genetics, Swedish Museum of Natural History, Stockholm, Sweden*

Corresponding author: Mariana P Braga, Department of Zoology, Stockholm University, Stockholm, SE-10691, Sweden; E-mail: mariana.braga@zoologi.su.se

1 *Abstract.*— Intimate ecological interactions, such as those between parasites and their hosts, may persist
2 over long time spans, coupling the evolutionary histories of the lineages involved. Most methods that
3 reconstruct the coevolutionary history of such associations make the simplifying assumption that parasites
4 have a single host. Many methods also focus on congruence between host and parasite phylogenies, using
5 cospeciation as the null model. However, there is an increasing body of evidence suggesting that the host
6 ranges of parasites are more complex: that host ranges often include more than one host and evolve via
7 gains and losses of hosts rather than through cospeciation alone. Here, we develop a Bayesian approach for
8 inferring coevolutionary history based on a model accommodating these complexities. Specifically, a
9 parasite is assumed to have a host repertoire, which includes both potential hosts and one or more actual
10 hosts. Over time, potential hosts can be added or lost, and potential hosts can develop into actual hosts or
11 vice versa. Thus, host colonization is modeled as a two-step process, which may potentially be influenced
12 by host relatedness or host traits. We first explore the statistical behavior of our model by simulating
13 evolution of host-parasite interactions under a range of parameters. We then use our approach,
14 implemented in the program RevBayes, to infer the coevolutionary history between 34 Nymphalini
15 butterfly species and 25 angiosperm families.
16 (Keywords: ancestral hosts, coevolution, herbivorous insects, probabilistic modeling.)

17 Extant ecological interactions, such as those between parasites and hosts, are often the
18 result of a long history of coevolution between the involved lineages (Elton 1946; Klassen 1992).
19 Specialization is predominant among parasites (including parasitic herbivorous insects; Forister
20 et al. 2015), but host associations are not static: they continuously evolve over time via gains and
21 losses of hosts (Janz and Nylin 2008; Nylin et al. 2018). The colonization of new hosts and loss of
22 old hosts not only shape the evolutionary trajectories of the interacting lineages, but can also
23 have large effects at ecological timescales (Nosil 2002; Calatayud et al. 2016). These effects are
24 evident, for example, with emerging infectious diseases and zoonotic diseases (Acha and Szyfres
25 2003), which involve colonization of new hosts within and among groups of domesticated species
26 (Subbarao et al. 1998), wildlife (Fisher et al. 2009), and humans (Hahn et al. 2000). Unraveling
27 the processes underlying changes in species associations is thus key to understanding evolutionary
28 and ecological phenomena at various timescales, such as the emergence of infectious diseases,
29 community assembly, and parasite diversification (Hoberg and Brooks 2015).

30 Many methods developed to study historical associations focus on congruence between
31 host and parasite phylogenies (Brooks 1979; Huelsenbeck et al. 1997; de Vienne et al. 2013). Such
32 methods largely fall into two main classes of cophylogenetic approaches: (1) topology- and
33 distance-based methods, which estimate the congruence between two phylogenies (Legendre et al.
34 2002), and (2) event-based methods, which map the parasite phylogeny onto the host phylogeny
35 using evolutionary events (Ronquist 2003). Typically, cospeciation is the null hypothesis in these
36 methods, where host shifts are invoked only to explain deviations from cospeciation (de Vienne
37 et al. 2013). Moreover, most of these methods do not allow ancestral parasites to be associated
38 with more than one host lineage, thus failing to account for a potentially important driver of
39 parasite diversification (Janz and Nylin 2008).

40 An alternative approach to studying coevolving host-parasite associations is to perform
41 ancestral state reconstructions of individual host taxa onto the parasite phylogeny and combine
42 the ancestral host states *a posteriori* into inferred host ranges (e.g. Nylin et al. 2014). Even
43 though this approach allows ancestral parasites to have multiple hosts, it assumes that the

44 associations between the parasite and each host evolve independently. This has a number of
45 serious drawbacks. For instance, ancestral parasites may be inferred to have an unrealistically
46 high number of hosts, or no host at all. Furthermore, the more narrowly circumscribed the host
47 taxa are, the more likely it is that ancestral parasite lineages are reconstructed as having no
48 hosts. In addition, the independence assumption causes the phylogenetic relationships among
49 hosts to be ignored, meaning that the model assigns equal rates to all colonizations of new hosts
50 regardless of how closely related the new host is to the current hosts being used by the parasite.

51 A desirable model of host usage should therefore allow parasites to have multiple hosts,
52 while also allowing for among-host (or context-dependent) effects to influence ancestral host use
53 estimates and gain and loss rates in whatever manner explains the biological data best. One
54 possible solution is to restate the problem of host-parasite co-evolution in terms of historical
55 biogeography. For instance, the Dispersal-Extirpation-Cladogenesis (DEC) model of Ree et al.
56 (2005) allows species ranges to stochastically evolve as a set of discrete areas over time through
57 area gain events (dispersal), area loss events (extirpation), and cladogenetic events (range
58 inheritance patterns that reflect speciation models). Although these methods are designed for
59 biogeographic inference, a similar approach is clearly suitable for more realistic modeling of
60 host-parasite coevolution dynamics, where colonization and loss of hosts (instead of discrete
61 areas) is modeled as a continuous-time Markov process (e.g. Hardy 2017). In biogeography, the
62 colonization of a new area or the disappearance from a previously occupied area is modeled as a
63 binary trait: the species is either present or absent in the area. While this binary view might be
64 simple but useful in biogeography, it may be too simplistic for use in the coevolution between
65 hosts and parasites. For instance, it is known that butterflies can utilize a range of plants that
66 they do not regularly feed on in the wild, and it has been suggested that these potential hosts
67 have played an important role in the evolution of host use in butterflies, by increasing the
68 variability in host use through time and across clades (Janz et al. 2016; Braga et al. 2018). This
69 hypothesis can only be directly tested, however, if we explicitly model the evolution of host use as
70 a two-step process, which cannot be done with the binary methods that are used today to study

71 host-parasite coevolution or biogeography.

72 Here, we propose a model where a parasite is assumed to have a *host repertoire*, defined as
73 the set of all potential and actual hosts for that parasite. In this model, the colonization of a new
74 host involves two steps: first, the parasite gains the ability to use the new host (it becomes a
75 potential host), and then starts actually using it in nature (it becomes an actual host). These two
76 steps can be interpreted as the inclusion of the new host into the fundamental and then into the
77 realized host repertoire of the parasite - analogous to fundamental and realized niche (Nylin et al.
78 2018; Larose et al. 2019). Similarly, the complete loss of a host from a parasite's realized
79 repertoire involves two steps. First, it changes from an actual to a potential host, and then it is
80 lost completely from the host repertoire. For example, if the geographic range of a host
81 contracted to become allopatric with respect to a parasite's geographic range, the host would
82 remain as part of the fundamental repertoire until the parasite completely lost the ability to use
83 the host, in which case the host would be lost from the repertoire. Even when in sympatry, the
84 evolution of a new defense mechanism by the host may prevent the parasite from using that host.
85 However, since host use is a complex and multidimensional trait, it is unlikely that a parasite
86 loses all the machinery necessary to use a host in one single event, and it may well retain some
87 ability to survive on the host. Thus, three host-parasite association states are necessary for such a
88 two-step model: the host is used (actual host), the parasite has some ability to use the host but
89 does not use it in nature (potential host), and the parasite cannot use the host (non-host).

90 In this paper, we develop a Bayesian approach to coevolutionary inference based on such a
91 model of host repertoire evolution, inspired by the previous work on similar biogeographic
92 inference problems by Landis et al. (2013). The basic binary biogeographic model, when applied
93 to coevolution, accommodates both multiple ancestral hosts and changes in host configurations
94 over time that correspond to evolutionary changes in host lineages or host traits. We extend this
95 model to also include a two-step host colonization process, such that the fundamental host
96 repertoire can persist over time and affect the evolution of the realized repertoire. We have
97 implemented the model in RevBayes (Höhna et al. 2016), allowing us to perform simulation as

98 well as Bayesian Markov chain Monte Carlo (MCMC) inference under the model. This Bayesian
99 framework allows one to estimate the joint distribution of host gain and loss rates, the effect (if
100 any) of phylogenetic distances among hosts upon host gain rates, and the historical sequences of
101 evolving host repertoires among the parasites. Using simulations, we explore the statistical
102 behavior of our approach, and demonstrate its empirical application with an analysis of the
103 coevolution between Nymphalini butterflies and their angiosperm hosts.

104 METHODS

105 *Model description*

106 We are interested in modeling the evolution of ecological interactions between M extant
107 parasite taxa and N host taxa, where each parasite uses one or more hosts. Rooted and
108 time-calibrated phylogenetic trees describe the evolutionary relationships among the M parasite
109 taxa and among the N host taxa. In this study, the trees are considered to be known without
110 error. In principle, it would be straightforward for the model to accommodate phylogenetic
111 uncertainty in the host or parasite trees but MCMC inference may prove challenging under such
112 conditions.

113 Each parasite taxon has a host repertoire, which is represented by a vector of length N
114 that contains the information about which hosts the given parasite uses. The interaction between
115 the m -th parasite and the n -th host is denoted $x_{m,n}$. At any given time, each host taxon can
116 assume one of three states with respect to a parasite lineage: $x_{m,n}$ is equal to 0 (non-host), 1
117 (potential host), or 2 (actual host). Criteria for how to code non-host, potential host, and actual
118 host states will depend on the host-parasite system under study; below, we provide criteria for
119 our Nymphalini dataset that may act as guidelines. We allow all host repertoires in which the
120 parasite has at least one actual host. Thus, the state space, S , includes $3^N - 2^N$ host repertoires
121 for N hosts.

122 Here we define the transition from state 0 to state 1 as the gain of the ability to use the
123 host, and the transition from state 1 to state 2 as the time when the parasite actually starts to
124 use the host in nature. If we assume that gains and losses of hosts occur according to a
125 continuous-time Markov chain, the probability of a given history of association between a parasite
126 clade and their hosts can be easily calculated (Ree and Smith 2008). This calculation is based on a
127 matrix, \mathbf{Q} , containing the instantaneous rates of change between all pairs of host repertoires, and
128 thus describing the Markov chain. Based on the \mathbf{Q} matrix, it is possible to calculate the transition
129 probability of the observed host repertoires at the tips of the parasite tree by marginalizing over
130 the infinite number of histories that could produce the observed host repertoires. Unfortunately,
131 computing these transition probabilities becomes intractable as the number of host repertoire
132 configurations, S , grows large. Modeling host repertoire evolution for host repertoire size $N = 7$
133 requires an $S \times S$ rate matrix defined for $S = 3^7 - 2^7 = 2059$, causing \mathbf{Q} to be too large for
134 efficient inference. In order to handle large host repertoires, we numerically integrate over possible
135 histories using data augmentation and MCMC rather than analytically computing the
136 probabilities using matrix exponentiation. This data augmentation approach has been used to
137 model sequence evolution for protein-coding genes (Robinson 2003) and historical biogeography
138 (Landis et al. 2013; Quintero and Landis 2019), suggesting the framework may be useful to model
139 host-parasite interactions as well. In this study, we assume that both daughter lineages identically
140 inherit their host repertoires from their immediate ancestor at the time of cladogenesis.

141 We define a model where the gain of a host (both $0 \rightarrow 1$ and $1 \rightarrow 2$) depends on the
142 phylogenetic distance between the available hosts and those currently used by a lineage. Figure 1
143 schematically illustrates the evolutionary dynamics of the model using $M = 4$ parasite species and
144 $N = 5$ host species, while assuming that host gain rates are independent (Fig. 1a,c) or dependent
145 (Fig. 1b,d) of phylogenetic distances among hosts. To formalize these dynamics, let $q_{\mathbf{y},\mathbf{z}}^{(a)}$ be the
146 rate of change from host repertoire \mathbf{y} to repertoire \mathbf{z} by changing the state of host a . Also, let λ_{ij}
147 be the rate at which an individual host changes from state i to state j , and $\eta(\mathbf{y}, a, \beta)$ be a
148 phylogenetic-distance rate modifier. The phylogenetic-distance rate modifier function, η , rescales

149 the base rate of host gain to allow new hosts that are closely related to the parasite's current
150 hosts to be colonized at higher rates than distantly related hosts. We define the instantaneous
151 rate of change as

$$q_{\mathbf{y},\mathbf{z}}^{(a)} = \begin{cases} \lambda_{10}, & \text{if potential host loss } (y_a = 1 \text{ and } z_a = 0) \\ \lambda_{01}\eta_1(\mathbf{y}, a, \beta) & \text{if potential host gain } (y_a = 0 \text{ and } z_a = 1) \\ \lambda_{21}, & \text{if actual host loss } (y_a = 2 \text{ and } z_a = 1) \\ \lambda_{12}\eta_2(\mathbf{y}, a, \beta) & \text{if actual host gain } (y_a = 1 \text{ and } z_a = 2) \\ 0, & \text{if direct transition between states 0 and 2 } (|y_a - z_a| > 1) \\ 0, & \text{if } \mathbf{y} \text{ and } \mathbf{z} \text{ differ at more than one host} \\ 0 & \text{if } \mathbf{z} \text{ does not contain at least one actual host} \end{cases}$$

152 and the phylogenetic-distance rate modifier function as

$$\eta(\mathbf{y}, a, \beta) = e^{-\beta d/\bar{d}}, \quad (1)$$

153 where β controls the effect of d , the average pairwise phylogenetic distance between the new host,
154 a , and the hosts currently occupied in \mathbf{y} ; and \bar{d} is the average phylogenetic distance between all
155 pairs of hosts. Pairwise phylogenetic distance is defined as the sum of branch lengths separating
156 two leaf nodes. The difference between η_1 and η_2 is that in the first, pairwise distances are
157 calculated between the new host and all potential and actual hosts, while in the second only
158 actual hosts are included. This allows for a model formulation where the effect of host distances
159 on λ_{01} and on λ_{12} are independent, while still allowing a formulation where they are equal. If
160 $\beta = 0$, the gain rate of host a is equal to the unmodified gain rate, λ_{01} or λ_{12} . If $\beta > 0$, the gain
161 rate of phylogenetically close hosts is higher than distant hosts.

162 We fit this model using the Bayesian data augmentation strategy described in Landis

163 et al. (2013). The method estimates the joint posterior probability of model parameters,
164 $\theta = (\mu, \lambda, \beta)$, and data-augmented evolutionary histories, X_{aug} , conditional on the observed host
165 repertoire data, X_{obs} , and the parasite phylogeny, Ψ_p , and the host phylogeny, Ψ_h , using MCMC.
166 To sample values from the posterior, $P(X_{\text{aug}}, \theta \mid X_{\text{obs}}, \Psi_p, \Psi_h)$, new parameter values for μ , λ , and
167 β are proposed using standard Metropolis-Hastings proposals for updating simple parameters
168 (Hastings 1970). Analogously, our MCMC stochastically proposes and/or accepts new augmented
169 host repertoire histories using the Metropolis-Hastings algorithm. Augmented histories are
170 proposed using two types of MCMC moves: branch-specific moves and node-and-branch moves.
171 Branch-specific moves propose a new augmented history by sampling a branch from the
172 phylogeny uniformly at random, then proposing new histories for a subset of host-characters using
173 the rejection sampling method of Nielsen (2002) under the assumption that all host characters
174 evolved under mutual independence ($\beta = 0$); this assumption allows us to rapidly propose new
175 augmented histories. Although augmented histories are proposed assuming host characters evolve
176 independently, we compute the acceptance probability for the branch-specific move by considering
177 the full-featured model probability that allows for non-independent rates of character change
178 when calculating the Metropolis-Hastings ratio. Thus, the augmented histories are sampled in
179 proportion to their posterior probabilities under the full model. Node-and-branch moves involves
180 sampling new host repertoire states for a node sampled uniformly at random within the parasite
181 tree, along with the three branches incident to the node. Together, the branch-specific moves, the
182 node-and-branch moves, and the parameter moves allow MCMC to estimate the posterior
183 probability of combinations of host repertoire histories and evolutionary parameters. Further
184 details are provided in Landis et al. (2013).

185 *Model selection*

186 When $\beta = 0$, the phylogenetic-distance dependent model, M_D becomes a mutual-independence
187 model, M_0 , where the interaction between the parasite and each host evolves independently.
188 These models are therefore nested ($M_0 \subseteq M_D$) and we can compute Bayes factors for model M_D

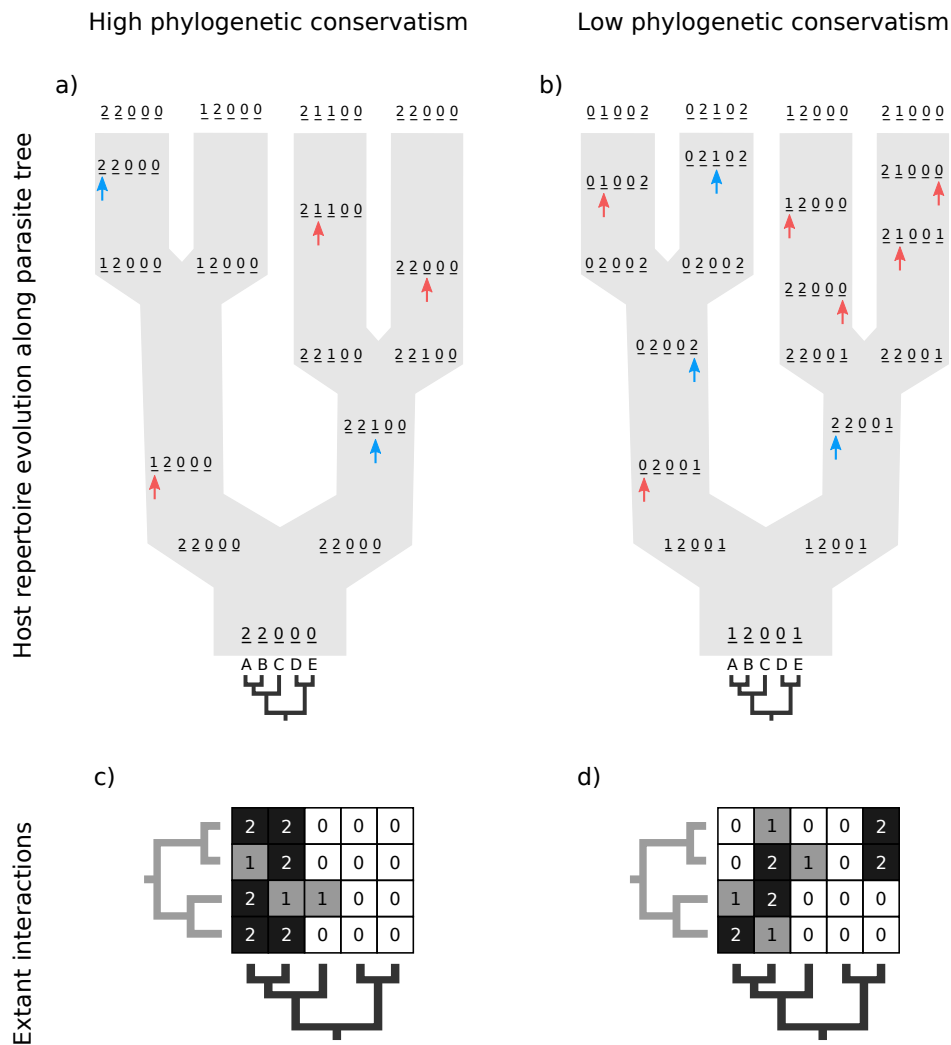


Figure 1: Host repertoire evolution along a hypothetical tree and resulting host-parasite interactions. Two examples of coevolutionary histories between four parasites and five hosts are shown to illustrate how the model works. Host repertoires evolve by gains ($0 \rightarrow 1$ and $1 \rightarrow 2$, blue arrows) and losses ($1 \rightarrow 0$ and $2 \rightarrow 1$, red arrows). Coevolutionary histories in **a** and **b** produce the interactions in **c** and **d** respectively. In **c** and **d**, each column represents one host and each row represents the host repertoire of one parasite. High phylogenetic conservatism is produced when the rate of repertoire evolution, μ , is low and the effect of the phylogenetic distance between hosts, β , is high. Conversely, low phylogenetic conservatism is produced when μ is high and β is low.

189 over model M_0 using the Savage-Dickey ratio (Verdinelli and Wasserman 1995; Suchard et al.
190 2001), defined as

$$B_{D,0} = \frac{P(\beta = 0 \mid M_D)}{P(\beta = 0 \mid \mathbf{x}_{\text{obs}}, M_D)} \quad (2)$$

191 where $P_D(\beta = 0 \mid M_D)$ is the prior probability and $P(\beta = 0 \mid \mathbf{x}_{\text{obs}}, M_D)$ is the posterior
192 probability, both defined in terms of the phylogenetic-distance dependent model, M_D , at the
193 restriction point $\beta = 0$ where M_D and M_0 are equivalent. While we could directly compute the
194 prior probability of $\beta = 0$, we approximated the posterior at $\beta = 0$ using a kernel density
195 estimator with a gamma function, which only takes positive values, and a bandwidth of 0.02. To
196 interpret if and how Bayes factors favored the phylogenetic-distance dependent model, M_D , we
197 followed the guidelines of Jeffreys (1961): model M_0 is favored for Bayes factors with values less
198 than 1, insubstantial support is awarded to model M_D for values between 1 and 3, substantial
199 support for values between 3 and 10, strong support for values between 10 and 30, very strong
200 support for values between 30 and 100, and decisive support for values greater than 100.

201

Data analysis

202 *Simulation study.*— We simulated 50 datasets for each of nine combinations of values for the rate
203 of host-repertoire evolution, μ (0.01, 0.04, and 0.1), and values of β (0, 1, and 4). These
204 parameter combinations produce datasets with varying degrees of phylogenetic conservatism for
205 both parasites and hosts (Fig. 2). Each dataset contained 34 insects and 25 hosts, and was
206 produced by simulating host repertoire evolution in the parasite tree used in the empirical study
207 (see below). Host gain and loss rates were chosen to resemble the rates inferred from the
208 empirical analysis. This simulation was designed to assess our statistical power to detect the
209 effect of phylogenetic distance among hosts upon host gain rates given the size of our empirical
210 dataset and the type of variation we expected it to contain.

211 We ran independent MCMC analyses for each set of 50 datasets, under the
212 phylogenetic-distance dependent model. We then quantified how well the posterior probabilities

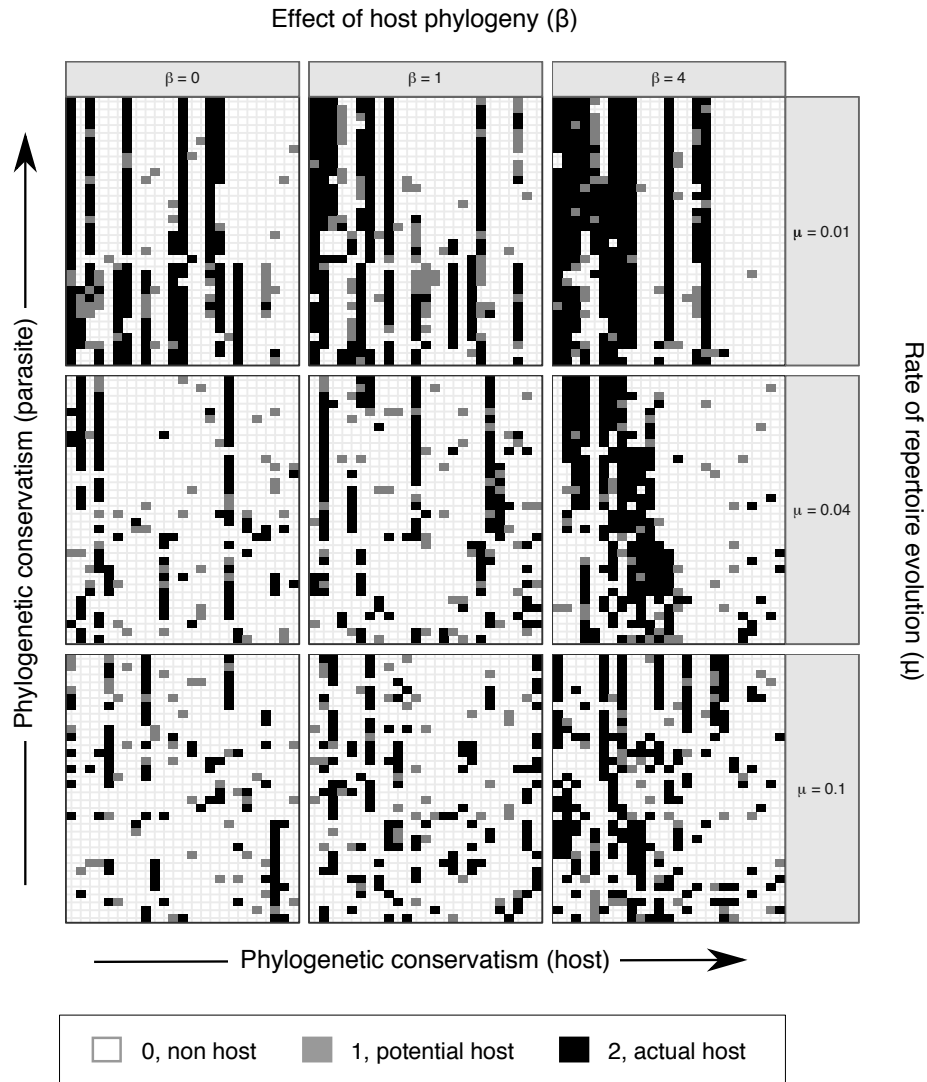


Figure 2: Simulated datasets for nine parameter combinations. Interactions between Nymphalini butterflies and their host plants for one of 50 simulations with each parameter combination. In each of the nine datasets, each column represents one host in the repertoire and each row shows the host repertoire of one butterfly species. When phylogenetic conservatism in host-parasite interactions is low for both hosts and parasites, the interactions are more randomly spread (matrix at bottom-left corner). As phylogenetic conservatism among parasites increases, host repertoires (rows) become more similar (upper matrices). When there is phylogenetic conservatism among hosts, host repertoires include more closely-related hosts (neighbouring columns; matrices to the right)

213 of coevolutionary histories correspond to the true history known from each simulation.
214 Specifically, we first computed the posterior probability of interaction between each host and each
215 internal node in the butterfly tree, for states 1 and 2 separately. Then, we calculated the sum of
216 squared differences between each posterior probability ($0 \leq P \leq 1$) and the corresponding truth
217 for that simulation (1, if the host was on the given state in the simulated dataset; 0, if not). This
218 error term increases as the inferred ancestral host repertoires become less accurate.

219 *Empirical study.*— In order to validate our method, we compiled data from the literature for
220 butterflies from the tribe Nymphalini (Nymphalidae) and their host plants (see Supplementary
221 Information for reference list). We chose this butterfly clade because we expect that a large
222 fraction of the real potential hosts are known, as there has been systematic experimental studies
223 of larval feeding ability. The dataset included 34 butterflies species and plants from 16
224 angiosperm families (Figs. S1 and S2). For each butterfly species, host plants commonly used in
225 nature were coded as ‘actual hosts’ and plants never used were coded as ‘non-hosts’. Plants that
226 are not commonly used in nature, but for which there is strong evidence (field observation or
227 experiment) that the larvae can feed upon them, were coded as ‘potential hosts’.

228 Because we lack the information on potential hosts for most host-parasite systems (i.e.
229 hosts are usually only classified as hosts or non-hosts), we tested whether our model is able to
230 recover the same parameter estimates and coevolutionary histories when all the potential hosts
231 are coded as non-hosts. For that, we ran the same analysis as for the full dataset, but first
232 removed all the 1s from the empirical dataset. Then we compared the posterior probabilities
233 inferred from the two datasets. To assess the similarities between the coevolutionary histories
234 inferred using the different datasets, we calculated summary statistics for the absolute difference
235 in probability of each interaction between hosts and internal nodes in the butterfly tree.

236 For both the simulation and empirical studies we used the phylogenetic relationships
237 between butterfly species in the Nymphalini tribe as proposed by Chazot (unpublished, Fig. S3)
238 and the phylogenetic relationships between angiosperm families proposed by Magallón et al.
239 (2015). Although our framework allows the inclusion of a large number of hosts in the same

240 analysis, computational time increases significantly with the size of the host repertoire. We
241 therefore chose to include 25 hosts, which allows the inclusion of all host lineages used by any of
242 the butterflies. To ensure the inclusion of all plant lineages that might have been used as hosts in
243 the past, we pruned the angiosperm phylogenetic tree so that all 16 families in the dataset were
244 included, and the remaining branches were collapsed to more ancestral nodes until only 25 tips
245 were left. We then pruned all the branches leading up to the tips to the time of origin of the
246 butterfly clade (approx. 22 Ma), and this pruned tree was then used to calculate phylogenetic
247 distances between hosts. To simplify the analysis, we hold the phylogenetic distances between
248 plant families constant, independent of geological time, even though the distances would be
249 expected to increase as evolution proceeds towards the recent.

250 We summarized inferred coevolutionary histories in two ways. First, we calculated the
251 posterior probability for fundamental and realized host repertoires at internal nodes of the
252 Nymphalini phylogeny based on the frequency with which states 1 and 2 were sampled for each
253 host during MCMC. Second, in order to reduce the dimensionality of the host repertoire and
254 facilitate visualization of ancestral state reconstructions, we assigned hosts to modules based on
255 extant butterfly-plant interactions (Fig. S2). Modules are groups of plants and butterflies that
256 interact more with each other than with other taxa, thus host plants are assigned to the same
257 module when they are used by the same butterflies. To identify the modules, we used a simulated
258 annealing algorithm that maximizes the index of modularity. Specifically, we used Newman and
259 Girvans metric (Newman and Girvan 2004) modified for bipartite networks (Barber 2007) as
260 implemented in the software MODULAR (Marquitti et al. 2014).

261 *Software configuration.*— All analyses were performed in RevBayes (Höhna et al. 2016). For the
262 simulated data, we ran two independent MCMC analyses for 10^5 cycles, sampling parameters and
263 node histories every 50 cycles, and discarding the first 5×10^4 as burnin. For the empirical data,
264 we ran five independent MCMC analyses, each set to run for 10^6 cycles, sampling every 50 cycles,
265 and discarding the first 10^5 as burnin. To verify that MCMC analyses converged to the same
266 posterior distribution, we applied the Gelman diagnostic (Gelman and Rubin 1992) provided

267 through the R package *coda* (Plummer et al. 2006). For both simulated and empirical datasets,
268 we used the following priors: $\beta \sim \text{Exponential}(1)$, $\mu \sim \text{Exponential}(10)$, and
269 $\lambda \sim \text{Dirichlet}(1, 1, 1, 1)$. Analysis scripts and data files are available at
270 https://github.com/mpiresbr/host_repertoire. A RevBayes tutorial for the empirical
271 analysis will be soon available at https://revbayes.github.io/tutorials#host_rep.

272

RESULTS

273 *Simulation study.*—Posterior distributions of parameter values for the 9×100 MCMC analyses are
274 shown in Figure 3. Overall, the model was able to accurately recover the true simulation
275 parameters (true value within 95% highest posterior density, or HPD). However, accuracy
276 decreased with increasing rate of host repertoire evolution, possibly due to character saturation.

277 We performed model selection based on Bayes factors. Considering that the prior
278 distribution is $\beta \sim \text{Exponential}(1)$, a high marginal posterior probability for $\beta = 0$ under M_D is
279 necessary to result in a Bayes factor < 1 and thus selection of M_0 . For simulations with $\beta = 0$,
280 the correct model, M_0 , was selected in more than 60% of the simulations, and most of the
281 remaining simulations gave insubstantial support to M_D (Fig. 4). When $\beta = 1$, Bayes factors
282 correctly selected M_D in the majority of cases, but strong support for M_D was only achieved in
283 simulations with $\beta = 4$, particularly when the rate of evolution was highest ($\mu = 0.1$).

284 We then compared the true coevolutionary history of each simulation to the corresponding
285 posterior distribution of the sampled coevolutionary histories (Fig. 5). The estimation error, that
286 is, the sum of squared differences between estimated and true coevolutionary histories, was very
287 low when the rate of host-repertoire evolution was lowest ($\mu = 0.01$), but also when the
288 phylogenetic-distance power was highest ($\beta = 4$). This means that accuracy in the estimation of
289 coevolutionary history increases with phylogenetic conservatism on both the butterfly and the
290 plant trees. Overall, error was higher on the estimation of actual hosts (state 2) than potential
291 hosts (state 1).

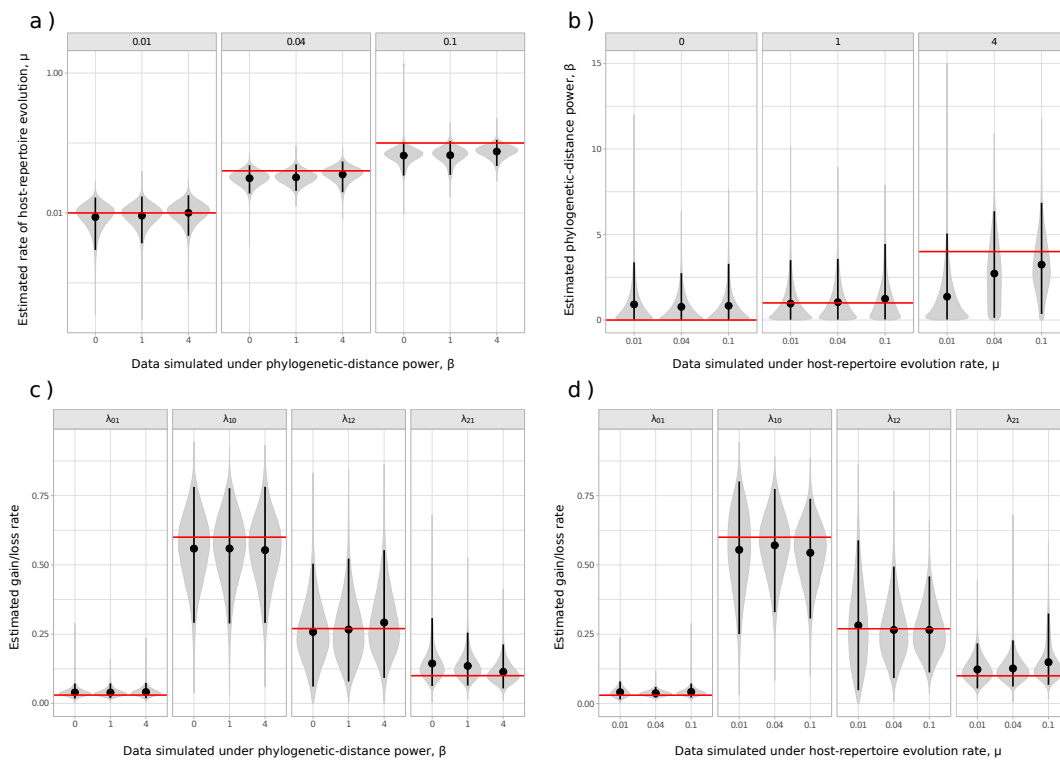


Figure 3: Posterior densities of parameters in the simulation study. Panels **a** and **b** are faceted by true parameter values of μ and β , respectively. Fifty datasets were simulated for each combination of $\beta \in \{0, 1, 4\}$ and $\mu \in \{0.01, 0.04, 0.1\}$, while $\lambda_{01} = 0.03$, $\lambda_{10} = 0.6$, $\lambda_{12} = 0.27$, and $\lambda_{21} = 0.1$ were held constant. For each parameter combination, the posterior distributions of the two MCMC samples of the 50 datasets were combined. Means are represented by black dots, black vertical lines show the 95% HPD, and red horizontal lines mark the true parameter value used in the simulations. Y-axis in panel **a** is in \log_{10} scale for better visualization.

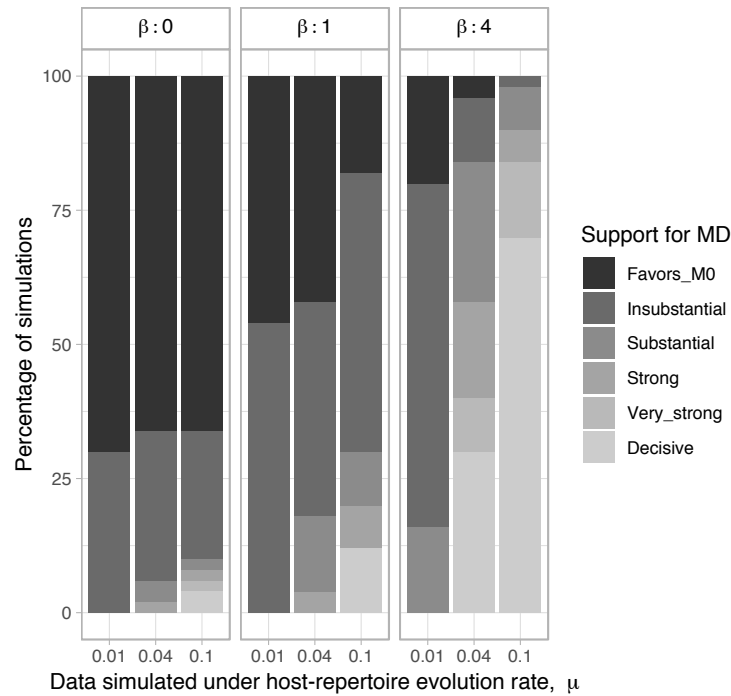


Figure 4: Distribution of Bayes factors for the simulation study. Each column corresponds to the strength of support per 2×50 MCMC analyses.

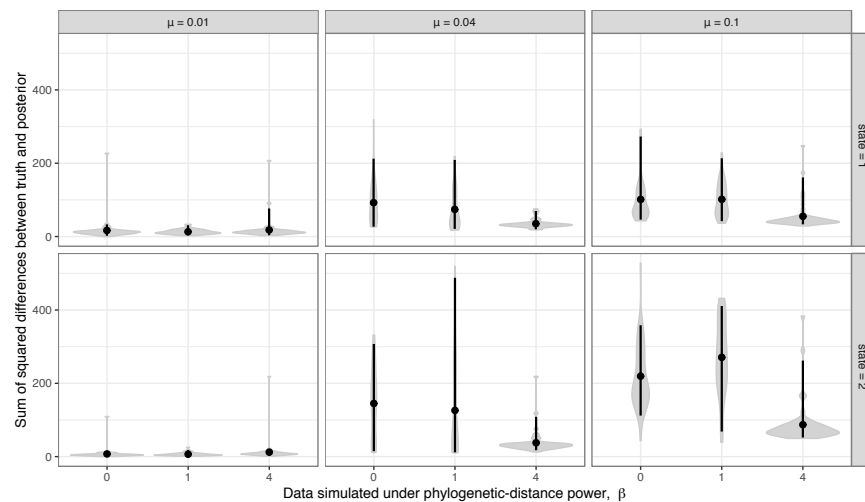


Figure 5: Errors for inferred dispersal histories of simulation study. The sum of squared differences between the posterior probability ($0 \leq P \leq 1$) and the true history ($P = 0$ or 1) for each host and each internal node were computed per simulated dataset. Each violin plot shows the distribution of these sums for each batch of 50 simulated datasets. Means are represented by black dots, black vertical lines show the 95% CI. Values of phylogenetic-distance power (β) are shown in the x-axis, columns are separated by the host-repertoire evolution rate (μ), and each row shows the error on the inference of each character state, i.e. potential host (1) or actual host (2).

292 *Empirical study.*— The estimated mean rate of host repertoire evolution for Nymphalini was
293 $\mu = 0.025$, the mean phylogenetic-distance power was $\beta = 0.51$, and the mean gain/loss rates were
294 $\lambda_{01} = 0.012$, $\lambda_{10} = 0.6$, $\lambda_{12} = 0.27$, and $\lambda_{21} = 0.12$ (Fig. 6, blue). Our method recovered similar
295 parameter estimates for the empirical dataset when omitting the intermediate state at the tips –
296 i.e. coding all potential hosts (state 1) as non-hosts (state 0): $\mu = 0.031$, $\beta = 0.39$, $\lambda_{01} = 0.001$,
297 $\lambda_{10} = 0.71$, $\lambda_{12} = 0.28$, and $\lambda_{21} = 0.01$ (Fig. 6, orange). The posterior distributions from analyses
298 with and without the intermediate state at the tips diverged the most for the rate parameters
299 associated with the transition to the intermediate state, λ_{01} and λ_{21} . In both cases the transition
300 rate was underestimated when 1s were removed from the dataset. Bayes factors selected the
301 independence model, M_0 , for both the full dataset (BF = 0.43) and when 1s were removed from
302 tip states (BF = 0.40).

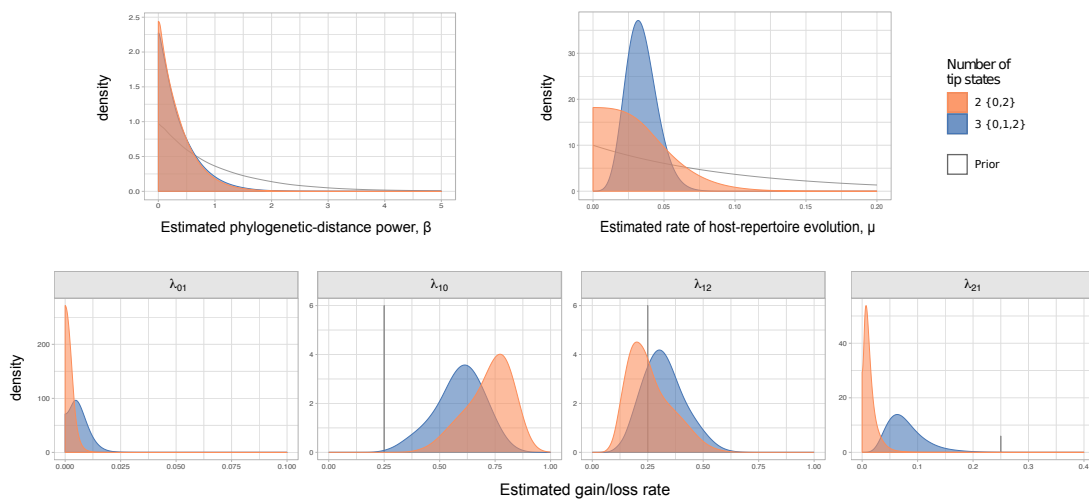


Figure 6: Marginal posterior densities for parameters in the Nymphalini-Angiosperms study for both the full dataset (3 states at tips) and the dataset omitting the intermediate state (2 states at tips). Grey lines corresponds to the priors $\beta \sim \text{Exponential}(1)$, $\mu \sim \text{Exponential}(10)$, and $\lambda \sim \text{Dirichlet}(1, 1, 1, 1)$.

303 Finally, we reconstructed the fundamental and realized host repertoires at internal nodes
304 of the Nymphalini phylogeny based on the sampled histories during MCMC. Coevolutionary
305 histories inferred using the datasets with and without potential hosts were very similar, with
306 mean difference in interaction probability of 0.003. Thus, we only show the ancestral states

307 inferred from the full, three-state dataset (Figs. 7 and S4). To facilitate visualization of the
 308 ancestral state reconstruction, we grouped the 16 parasitized host families into five modules, as
 309 identified by the simulated annealing algorithm (Fig. S2). Nine families (representing three
 310 modules) were inferred to be used by ancestral Nymphalini species with high probability.

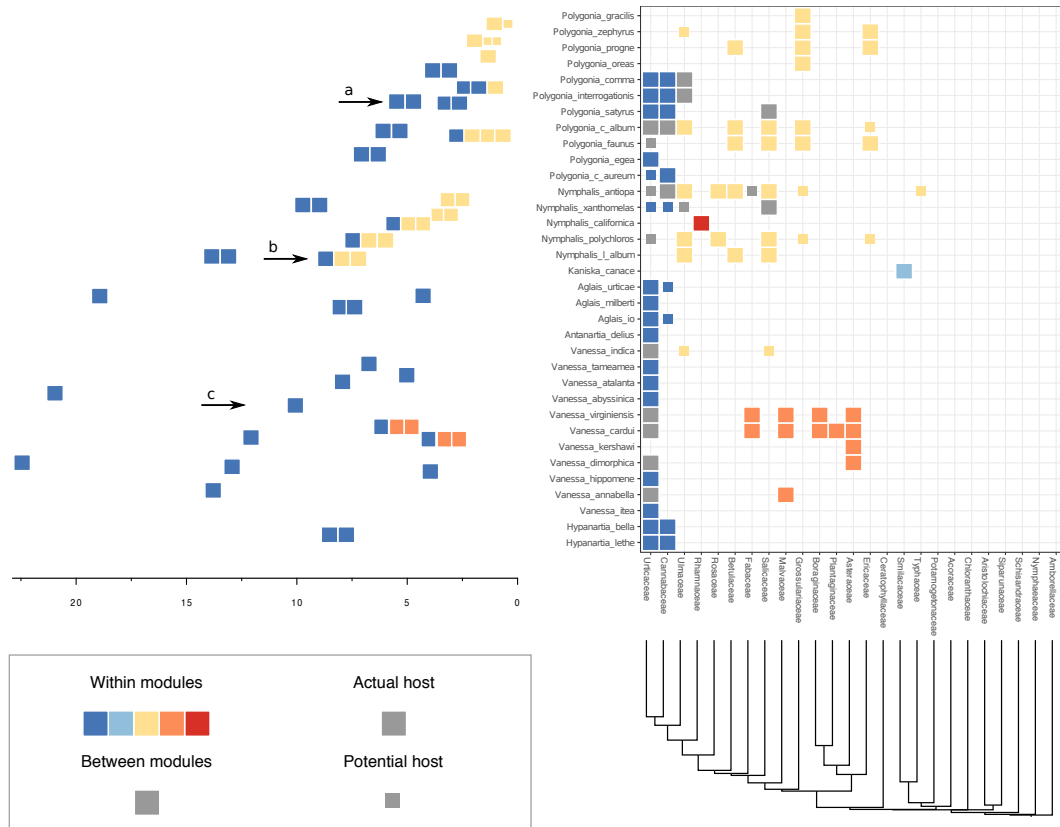


Figure 7: Evolution of butterfly-plant interactions through time. Ancestral state estimates (left) of host repertoire across the Nymphalini phylogeny are shown for interactions with more than 75% posterior probability. The x-axis under shows time before present in millions of years. Extant species interactions (right) between Nymphalini and their host plants are presented as a raster, where each square represents one interaction between a butterfly species and a host family. Colors represent different modules, i.e. groups of plants that are often hosts to the same butterflies at present time. Square size was used to differentiate between actual and potential hosts. Arrows indicate nodes shown in Fig. 8.

311 We found strong support for the association between the ancestor of all Nymphalini
 312 butterflies and Urticaceae hosts (and Cannabaceae to a lesser degree, Fig. S4). All other host

313 families have been colonized in the last 15 Myr, after the divergence of the two largest clades
 314 within Nymphalini, *Vanessa* and *Nymphalis* + *Polygonia*. Most species within *Vanessa*, both
 315 extant and ancestral, are specialists on Urticaceae. *V. virginiensis* and *V. cardui* are the only
 316 extant species that use more than two host families, and these hosts have likely been colonized by
 317 their most recent common ancestor (node 38 in Fig. 8). On the other hand, the variation in host
 318 use in the *Nymphalis* + *Polygonia* clade seems to be the result of host colonizations by multiple
 319 species along the diversification of the clade. For example, in Fig. 8 we can see the colonization of
 320 potential hosts by the ancestor of *P. c-album* and *P. faunus* (node 53) as well as strong
 321 specialization on a new host by *Kaniska canace*.

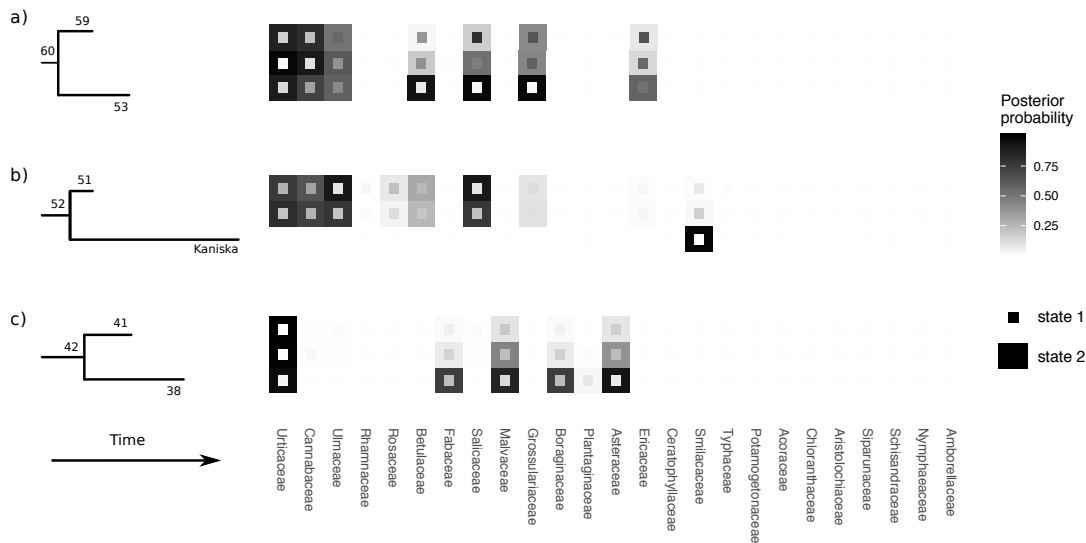


Figure 8: Host repertoires at selected nodes of the Nymphalini tree (arrows in Fig. 7). Numbers indicate the node index (compatible with Fig. S3). For the only terminal taxa depicted, *Kaniska canace*, the observed host repertoire is shown. For all other repertoires, the posterior probabilities for states 1 and 2 are shown.

322

DISCUSSION

323 The method we develop here to infer the evolutionary history of host-parasite associations
 324 has many advantages over previous approaches. First, it is based on stochastic models and on
 325 established principles of statistical inference, which means that it provides a robust framework for

326 characterizing the evolutionary processes that shape host-parasite associations and for selecting
327 among alternative coevolutionary models. Second, our model introduces the novel concept of a
328 host repertoire, which we think is an important step forward. Besides accounting for the
329 possibility of parasites having more than one host over time scales of macroevolutionary
330 significance, we can now directly infer the influence of host relatedness and host traits on the
331 process of gaining new hosts. Third, the stochastic model of host-parasite coevolution that we
332 introduce here is, to our knowledge, the first that explicitly accounts for evolution of the
333 fundamental host repertoire. By recognizing the fact that a parasite may have potential hosts in
334 addition to its actual hosts, and that the set of potential hosts may persist over time, the dynamic
335 of the model changes. What would otherwise have appeared as remarkable repeated patterns of
336 colonization of the same host lineages can now be explained as the effect of frequent transitions
337 between potential and actual hosts in an otherwise conserved host repertoire.

338 Our model can readily be extended in many interesting ways. The version we present here
339 accounts for the effect of host phylogeny by allowing the rate of host gain to depend on host
340 relatedness. For simplicity, we assumed that the number of available hosts and host relatedness
341 remain constant over geological time. This would be appropriate for a group of parasites that
342 radiated after the relevant host lineages had been formed, which is arguably the case for the
343 empirical example we chose. However, it should be relatively straightforward to extend our
344 framework to account for more complex dependencies on host phylogeny. For instance, the host
345 configurations could be modeled as changing over time, reflecting host cladogenesis.

346 Another interesting direction for future research would be to modify the particular ways in
347 which hosts and parasites coevolve. We note, for example, that Fig. 7 shows that host repertoires
348 of *Vanessa* species overlap very little with the host repertoires of *Nymphalis* + *Polygonia* species,
349 but it is not immediately clear what drives this pattern. One could design a model that allows the
350 rates of host gain and loss to be influenced by evolving host traits — like secondary metabolites,
351 growth form, or phenology, to mention a few examples relevant for insect-host plant associations
352 — in addition to relatedness among hosts. Or, one might extend the model to allow closely

353 related parasite lineages to competitively exclude one another from host usage, similar to how
354 competing lineages might exclude one another from geographical regions (Quintero and Landis
355 2019). Finally, one might introduce a biogeographical component to the coevolutionary process,
356 requiring parasites to be in sympatry with their actual hosts, while allowing parasites to be in
357 sympatry or allopatry with their potential hosts. Statistically comparing such model variants will
358 help illuminate drivers of host-parasite co-evolution.

359 A potential concern with our approach is that already the basic version of the model is
360 fairly parameter-rich. Given the type and amount of data that we can likely collect on
361 host-parasite associations, is there enough statistical power to select among the models of interest?
362 And is it possible to infer the model parameters of interest with a reasonable degree of accuracy?

363 Overall, our results are encouraging in this respect. The simulations indicate that it is
364 possible to infer the true parameter values of the basic model regardless of the level of
365 phylogenetic conservatism in both parasites and hosts (Fig. 3). When the rates of colonization of
366 new hosts are strongly dependent on the phylogenetic relatedness of hosts, then we are also able
367 to distinguish between models with or without host relatedness effects using Bayes factors (Fig.
368 4). However, our ability to select the correct model decreases when the effect of host phylogenetic
369 relatedness is low ($\beta \leq 1$), that is, when models become more similar. Further studies will have to
370 show to what extent the sensitivity of the model test can be increased by selecting appropriate
371 priors and improving the sampling of parameter space close to the boundary condition satisfying
372 the restricted model. One option is to relax the assumption that β is non-negative, which would
373 simplify the sampling of values close to $\beta = 0$. It will also be important to explore how dataset
374 sizes and tree shapes, for both hosts and parasites, influence our ability to distinguish the models
375 when the effect of host phylogeny is small.

376 Importantly, the empirical analysis indicates that the method is able to model the
377 evolution of fundamental and realized host repertoires even when the information about potential
378 hosts is lacking. This significantly increases the applicability of our method, as information about
379 fundamental host repertoires is missing for most host-parasite systems. Potential host data is

380 difficult to collect, as it requires experimental testing of a large number of potential host-parasite
381 pairs. A possible improvement of our method, which we did not explore here, would be to model
382 uncertainty in the observations of non-hosts when data on potential hosts are missing. That is, if
383 we had no information about a host species being used by a particular parasite, we would
384 translate that to a certain probability p of the species actually being a non-host, and a
385 complementary probability $1 - p$ of it being a potential host (Kuhner and McGill 2014). Modeling
386 this observational uncertainty could help reduce the bias in parameter estimates that we observed
387 when data on potential hosts were missing and all 0 states in the dataset were inappropriately
388 treated as true non-hosts. This extension would also allow us to make predictions about host use
389 abilities in extant parasites. These predictions could then inform experiments that aim to
390 characterize fundamental host repertoires.

391 We demonstrated the empirical application of our approach with a Bayesian inference of
392 the coevolutionary history between 34 Nymphalini butterflies and 25 angiosperm families. We
393 estimated the rate of host repertoire evolution along each branch of the butterfly tree as being
394 between 0.33 and 0.93 events per million years. Bayes factors favored the independence model,
395 where the probability of gaining a given hosts is not affected by the phylogenetic distance between
396 hosts. As explained above, this does not necessarily mean that host relatedness plays no role, only
397 that the effect is not large enough for us to detect it with the current approach and the given data.

398 Estimates of gain and loss rates were not symmetric, and the rates also varied between
399 states. According to our results, gain of the ability to use a host, λ_{01} , is very rare (0.5% to 1.9%
400 of overall rate), whereas loss is common (47% to 73% of overall rate). On the other hand,
401 transition rates between states 1 and 2 were more symmetric and gain is more common than loss
402 (λ_{12} between 15% and 39%; λ_{21} between 6% and 18% of overall rate). These rate estimates
403 support the idea that the use of the same host lineage by multiple, phylogenetically widespread
404 butterfly lineages is more likely explained by recolonization of hosts that have been used in the
405 past (recurrence homoplasy), that is, by transitions between actual and potential hosts, rather
406 than by completely independent colonizations of the same host (Janz et al. 2001). Note that

407 alternative scenarios that have been proposed in the literature to explain the evolution of
408 Nymphalini host plant preferences, for instance by involving narrow ancestral host plant ranges
409 and repeated independent colonization events, are also allowed by our model, but they are
410 inferred to be much less likely than the conservative host repertoire scenario. Yet, because the
411 potential host state is exited at the highest rate, the rate estimates also suggest that parasites do
412 not retain their potential host relationships for prolonged periods of time. The moderate rates of
413 transitions between potential and actual host states and the high departure rate from the
414 potential host state together help explain why phylogenetic “pulses” of recurrent host acquisition
415 manifest in some lineages but not others.

416 For example, the use of Grossulariaceae by two non-sister clades within *Polygonia* is best
417 explained by a scenario where Grossulariaceae was a potential host for the ancestral species (node
418 60 in Fig. 8) and was subsequently gained as an actual host twice (at nodes 53 and 58, Fig. S4).
419 The ability to use Salicaceae host plants seems to be even older. Salicaceae was likely a potential
420 host for the ancestor of *Nymphalis* + *Polygonia* and later became an actual host in three different
421 parts of the clade. If potential hosts were not explicitly modeled here, these transitions would
422 look like three independent colonizations of a plant group that is very distant from the ancestral
423 host (Salicaceae and Urticaceae diverged about 90 Ma). Instead, we could show that what might
424 appear as big and sudden host shifts, are in fact the result of retention of ancestral host use
425 abilities.

426 Understanding how ecological interactions change is crucial if we want to predict both
427 short and long-term consequences of global mixing of biota (Hoberg and Brooks 2015).
428 Host-parasite interactions are of particular interest given the risk of emerging diseases, which can
429 affect human populations directly and indirectly through their effects on crop species and wildlife
430 (Brooks et al. 2014). Our method was designed to quantify changes in host-parasite associations
431 by modeling the process of gaining and losing hosts, thus allowing us to make predictions based
432 on host-parasite history. Hopefully, our approach will not only generate deeper insights into the
433 evolutionary dynamics of host-parasite associations but also help humankind mitigate some of the

434 risks incurred by current environmental change.

435

FUNDING

436 M.J.L. was supported by the Donnelley Fellowship through the Yale Institute of Biospheric
437 Studies, with early work in this study supported by the NSF Postdoctoral Fellowship in Biology
438 (DBI-1612153). The Swedish Research Council supported SN (2015-04218) and FR (2014-05901).

439

*

440 Acha, P. N. and B. Szyfres. 2003. Zoonoses and communicable diseases common to man and
441 animals vol. 580. Pan American Health Org.

442 Barber, M. J. 2007. Modularity and community detection in bipartite networks. Physical review.
443 E, Statistical, nonlinear, and soft matter physics 76:066102.

444 Braga, M. P., P. R. Guimarães Jr, C. W. Wheat, S. Nylin, and N. Janz. 2018. Unifying
445 host-associated diversification processes using butterfly-plant networks. Nature communications
446 9.

447 Brooks, D. R. 1979. Testing the Context and Extent of Host-Parasite Coevolution. Systematic
448 Biology 28:299–307.

449 Brooks, D. R., E. P. Hoberg, W. A. Boeger, S. L. Gardner, K. E. Galbreath, D. Herczeg, H. H.
450 Mejia-Madrid, S. E. Racz, and A. T. Dursahinhan. 2014. Finding Them Before They Find Us:
451 Informatics, Parasites, and Environments in Accelerating Climate Change. Comparative
452 Parasitology 81:155–164.

453 Calatayud, J., J. L. Hórreo, J. Madrigal-González, A. Migeon, M. Á. Rodríguez, S. Magalhães,
454 and J. Hortal. 2016. Geography and major host evolutionary transitions shape the resource use
455 of plant parasites. Proceedings of the National Academy of Sciences 113:201608381–9845.

- 456 de Vienne, D. M., G. Refregier, M. Lopez-Villavicencio, A. Tellier, M. E. Hood, and T. Giraud.
457 2013. Cospeciation vs host-shift speciation: methods for testing, evidence from natural
458 associations and relation to coevolution. *New Phytologist* 198:347–385.
- 459 Elton, C. 1946. Competition and the Structure of Ecological Communities. *Journal of Animal*
460 *Ecology* 15:54–68.
- 461 Fisher, M. C., T. W. Garner, and S. F. Walker. 2009. Global emergence of *Batrachochytrium*
462 *dendrobatidis* and amphibian chytridiomycosis in space, time, and host. *Annual Review of*
463 *Microbiology* 63:291–310.
- 464 Forister, M. L., V. Novotny, A. K. Panorska, L. Baje, Y. Basset, P. T. Butterill, L. Cizek, P. D.
465 Coley, F. Dem, I. R. Diniz, P. Drozd, M. Fox, A. E. Glassmire, R. Hazen, J. Hrcek, J. P.
466 Jahner, O. Kaman, T. J. Kozubowski, T. A. Kursar, O. T. Lewis, J. Lill, R. J. Marquis, S. E.
467 Miller, H. C. Morais, M. Murakami, H. Nickel, N. A. Pardikes, R. E. Ricklefs, M. S. Singer,
468 A. M. Smilanich, J. O. Stireman, S. Villamarín-Cortez, S. Vodka, M. Volf, D. L. Wagner,
469 T. Walla, G. D. Weiblen, and L. A. Dyer. 2015. The global distribution of diet breadth in insect
470 herbivores. *Proceedings of the National Academy of Sciences* 112:442–447.
- 471 Gelman, A. and D. B. Rubin. 1992. Inference from Iterative Simulation Using Multiple Sequences.
472 *Statistical Science* 7:457–472.
- 473 Hahn, B. H., G. M. Shaw, K. M. De Cock, and P. M. Sharp. 2000. Aids as a zoonosis: scientific
474 and public health implications. *Science* 287:607–614.
- 475 Hardy, N. B. 2017. Do plant-eating insect lineages pass through phases of host-use generalism
476 during speciation and host switching? Phylogenetic evidence. *Evolution* 71:2100–2109.
- 477 Hastings, W. K. 1970. Monte Carlo sampling methods using Markov chains and their
478 applications. *Biometrika* 57:97–109.
- 479 Hoberg, E. P. and D. R. Brooks. 2015. Evolution in action: climate change, biodiversity dynamics

- 480 and emerging infectious disease. *Philosophical transactions of the Royal Society of London.*
481 *Series B, Biological sciences* 370:–20130553.
- 482 Höhna, S., M. J. Landis, T. A. Heath, B. Boussau, N. Lartillot, B. R. Moore, J. P. Huelsenbeck,
483 and F. Ronquist. 2016. RevBayes: Bayesian Phylogenetic Inference Using Graphical Models
484 and an Interactive Model-Specification Language. *Systematic Biology* 65:726–736.
- 485 Huelsenbeck, J. P., B. Rannala, and Z. H. Yang. 1997. Statistical tests of host-parasite
486 cospeciation. *Evolution* 51:410–419.
- 487 Janz, N., M. P. Braga, N. Wahlberg, and S. Nylin. 2016. On oscillations and flutterings—A reply
488 to Hamm and Fordyce. *Evolution* 70:1150–1155.
- 489 Janz, N., K. Nyblom, and S. Nylin. 2001. Evolutionary dynamics of host-plant specialization: a
490 case study of the tribe Nymphalini. *Evolution* 55:783–796.
- 491 Janz, N. and S. Nylin. 2008. The oscillation hypothesis of host-plant range and speciation.
492 Pages 203–215 *in* Specialization, speciation, and radiation: the evolutionary biology of
493 herbivorous insects (K. J. Tilmon, ed.). California Univ. Press, California.
- 494 Jeffreys, H. 1961. *The Theory of Probability*. OUP Oxford.
- 495 Klassen, G. J. 1992. Coevolution: A History of the Macroevolutionary Approach to Studying
496 Host-Parasite Associations. *The Journal of Parasitology* 78:573.
- 497 Kuhner, M. K. and J. McGill. 2014. Correcting for sequencing error in maximum likelihood
498 phylogeny inference. *G3: Genes, Genomes, Genetics* 4:2545–2552.
- 499 Landis, M. J., N. J. Matzke, B. R. Moore, and J. P. Huelsenbeck. 2013. Bayesian analysis of
500 biogeography when the number of areas is large. *Systematic Biology* 62:789–804.
- 501 Larose, C., S. Rasmann, and T. Schwander. 2019. Evolutionary dynamics of specialisation in
502 herbivorous stick insects. *Ecology Letters* 22:354–364.

- 503 Legendre, P., Y. Desdevises, and E. Bazin. 2002. A Statistical Test for Host–Parasite Coevolution.
504 *Systematic Biology* 51:217–234.
- 505 Magallón, S., S. Gómez-Acevedo, L. L. Sánchez-Reyes, and T. Hernández-Hernández. 2015. A
506 metacalibrated time-tree documents the early rise of flowering plant phylogenetic diversity.
507 *New Phytologist* 207:437–453.
- 508 Marquitti, F. M. D., P. R. Guimarães, M. M. Pires, and L. F. Bittencourt. 2014. MODULAR:
509 software for the autonomous computation of modularity in large network sets. *Ecography*
510 37:221–224.
- 511 Newman, M. E. J. and M. Girvan. 2004. Finding and evaluating community structure in
512 networks. *Physical review. E, Statistical, nonlinear, and soft matter physics* 69:026113.
- 513 Nielsen, R. 2002. Mapping Mutations on Phylogenies. *Systematic Biology* 51:729–739.
- 514 Nosil, P. 2002. Transition rates between specialization and generalization in phytophagous insects.
515 *Evolution* 56:1701–1706.
- 516 Nylin, S., S. Agosta, S. Bensch, W. A. Boeger, M. P. Braga, D. R. Brooks, M. L. Forister, P. A.
517 Hambäck, E. P. Hoberg, T. Nyman, A. Schäpers, A. L. Stigall, C. W. Wheat, M. Österling, and
518 N. Janz. 2018. Embracing Colonizations: A New Paradigm for Species Association Dynamics.
519 *Trends in Ecology & Evolution* 33:4–14.
- 520 Nylin, S., J. Slove, and N. Janz. 2014. Host plant utilization, host range oscillations and
521 diversification in nymphalid butterflies: a phylogenetic investigation. *Evolution* 68:105–124.
- 522 Plummer, M., N. Best, K. Cowles, K. Vines, and 2006. 2006. CODA: convergence diagnosis and
523 output analysis for MCMC. *R News* 6:7–11.
- 524 Quintero, I. and M. J. Landis. 2019. Interdependent Phenotypic and Biogeographic Evolution
525 Driven by Biotic Interactions. *BioRxiv* Page 560912.

- 526 Ree, R. H., B. R. Moore, C. O. Webb, and M. J. Donoghue. 2005. A likelihood framework for
527 inferring the evolution of geographic range on phylogenetic trees. *Evolution* 59:2299–2311.
- 528 Ree, R. H. and S. A. Smith. 2008. Maximum likelihood inference of geographic range evolution by
529 dispersal, local extinction, and cladogenesis. *Systematic Biology* 57:4–14.
- 530 Robinson, D. M. 2003. Protein Evolution with Dependence Among Codons Due to Tertiary
531 Structure. *Molecular Biology and Evolution* 20:1692–1704.
- 532 Ronquist, F. 2003. Parsimony analysis of coevolving species associations . Pages 22–64 *in* Tangled
533 trees: Phylogeny, cospeciation and coevolution. (R. D. M. Page, ed.). University of Chicago
534 Press, Chicago.
- 535 Subbarao, K., A. Klimov, J. Katz, H. Regnery, W. Lim, H. Hall, M. Perdue, D. Swayne,
536 C. Bender, J. Huang, et al. 1998. Characterization of an avian influenza A (H5N1) virus
537 isolated from a child with a fatal respiratory illness. *Science* 279:393–396.
- 538 Suchard, M. A., R. E. Weiss, and J. S. Sinsheimer. 2001. Bayesian selection of continuous-time
539 Markov chain evolutionary models. *Molecular Biology and Evolution* 18:1001–1013.
- 540 Verdinelli, I. and L. Wasserman. 1995. Computing Bayes Factors Using a Generalization of the
541 Savage-Dickey Density Ratio. *Journal of the American Statistical Association* 90:614–618.